In: TMS 2025: 154th Annual Meeting & Exhibition Supplemental Proceedings, Las Vegas, Nevada, USA. The Minerals, Metals & Materials Series, Springer Nature Switzerland, 2025, pp. 1352-1363
DOI:10.1007/978-3-031-80748-0_119

Impact of Cold-Wire Gas Metal Arc Welding (CW-GMAW) Parameters on Microstructure and Microhardness Characteristics in Repairing S275JR Structural Steel.

Zahraddeen Musa*, Supriyo Ganguly, Wojciech Suder, Victor Igwemezie, Kuladeep Rajamudili

Welding and Additive Manufacturing Centre, Building 46, Cranfield University, Cranfield MK43 0AL, UK

* Corresponding author: Zahraddeen.musa@cranfield.ac.uk

Abstract

This study investigates the influence of adding a cold wire during gas metal arc welding (CW-GMAW) for repair of S275JR structural steel. The research is aimed at improving repair productivity through increased deposition rates with enhanced performance.

During weld repair, multiple passes induce large number of thermal cycles and a huge thermal gradient on the material which has an adverse effect on the material's properties. This is largely due to the microstructural changes that occur during the process. In this work, a systematic approach has been adopted to explore the effects of varying gas metal arc welding (GMAW) parameters, including wire feed rate, welding current, voltage, travel speed, and specifically cold-wire feed speed on the heat affected zone (HAZ) microstructure and hardness.

Macrostructural examination highlights significant alterations in the heat-affected zone (HAZ) region, with marked microhardness changes in both WM and HAZ. Cold-wire addition led to a reduction in the HAZ area, depth of weld metal penetration, and significantly reduced the impact of imposing thermal cycles on the HAZ of the welded samples. Additionally, microstructural analysis was conducted using a standard optical microscope to correlate the observed hardness variations with microstructural transformations in the weld metal and heat-affected zone (HAZ).

The findings reveal that specific combinations of CW-GMAW parameters can significantly influence the microstructure and thereby hardness, suggesting that with careful control of these parameters, it would be possible to do faster repair with minimal loss of integrity for critical structural steels.

Keywords: Weld repair productivity, High deposition rate, Cold-wire Gas Metal Arc Welding (CW-GMAW)

1. Introduction

S275JR steel is a low carbon, mild steel grade that is a commonly used structural material for the heavy machinery in construction and transportation sectors. It possesses excellent properties, such as high strength, toughness, and good weldability. However, any imperfection in; the steel, may result in deterioration in the properties and eventually a severe failure at an unexpected time. Very often, the failure starts at welds that are used to join different sections of the steels. For the faulty components, replacement is a better solution but not economical always. As an alternative, repair and most probably repair through welding is easy and reliable (Yuhui *et al*., 2012) [1].

Repairs are interventions that aim to provide partial or total restoration of the operational capacity of the component at specific points due to the presence of damage (leaks, ruptures, dents, cracks etc.) (Sanchez *et al* 2017) [2]. The material to be welded and the welding process being used are the factors of highest concern.

Repairs of welds repeated in the same location is often carried out, but studies show that repeated thermal cycles could have an adverse effect on the material properties which will lead to total failure. In 10% sulphuric acid concentrated solution, corrosion susceptibility of the weld joint in X52 steel pipe was found increasing with the increase in number of repairs. It is caused by the higher level of residual stresses with multi repair of weld (Abbas, 2013) [3]. It is observed that in welded structures, weld metal and heat affected zone (HAZ) are the most prone locations for failure. Among various causes of failure, corrosion, hydrogen embrittlement, and residual stresses are topmost. All these issues will become even more prominent when multiple repairs are performed on these structural steels.

The status of research for microstructural characteristics of steels during welding applications indicated that various researchers have investigated the failure phenomena to find out their possible cause. However, studies on how repair welding damages these steels with regards to the degradation mechanisms that become active during

the repair is scanty. The quantification of the microstructural alterations in the HAZ of these steels by variation of the process parameters and resulting heat input during repair welding needs to be done. The proposed research intends to address this by using a novel approach of adding a cold wire for the repair welding of these structural steels. This will be effective in reducing the heat input, minimize residual stresses in the welded zone and develop a refined microstructure at the HAZ.

2. Materials and Methods

2.1 Sample Preparation and Welding

V-grooves with a 90 degrees angle and 10mm depth were gouged out from the S275JR steel plate substrate (20mm x 120mm x 70mm) to simulate the procedures for carrying out a weld repair. The gouging of these grooves was performed under low-speed conditions to prevent damage to the parent metal that could potentially alter its inherent microstructure. The substrates were thoroughly cleaned with wire brush, acetone, and paper to eliminate surface impurities before the deposition. The chemical compositions of the steel substrate and consumable electrodes are given in Table 1.

Table 1. Chemical composition of the steel substrate and welding wire in wt. (%).

Material	C	Mn	Si	Cr	Ni	Mo	P	S	Ni	Al	N	Cu	Fe
S275JR	0.14	1.1	0.24	0.24	0.03	0.005	0.013	0.002	0.03	0.044	0.006	0.03	Bal
ER70S-6	0.08	1.46	0.85	-	-	-	-	-	-	-	-	-	Bal

The cold-wire GMAW (CW-GMAW) process was employed to prepare the weld samples with cold wire feed rates of 0m/min, 5m/min and 10m/min, which will henceforth be referred to as CW0, CW5 and CW10 samples, respectively. For all the samples, a hot wire feed rate of 11m/min was maintained throughout the welding process. This ensured that the arc energy used (current and voltage) during the welding was kept constant. The welding conditions are presented in Table 2.

Table 2. Gas Metal Arc Welding Process Parameters

Process Parameter	Unit	Set Value		
Average Current	A	360		
Average Voltage	V	35		
Travel speed	m/min	0.47 (CW0)	0.65 (CW5)	0.82 (CW10)
Hot wire feed rate	m/min	11		
Cold wire feed rate	m/min	0 (CW0)	5 (CW5)	10 (CW10)

To ensure a controlled welding environment, a Fronius CMT Advanced 4000R power source, and a shielding gas mixture of 2.5% CO2 and 97.5% Argon (BOC Spec shield gas) at a flow rate of 18 l/min were used. ER70S-6 solid mild steel wire with a diameter of 1.2mm was used as the welding electrode (hot wire) and cold wire. The electrical signals during welding (arc current and voltage), were recorded using an arc monitor (AMV 4000), while a welding camera (Xiris type) provided real-time monitoring of the metal transfer, arc characteristics and the melt pool. The physical setup included attaching the steel plate substrate to a workbench with g-clamps and utilizing a 6-axis KUKA robot to automate the torch movement and deposit the weld accordingly. A contact tip to workpiece distance (CTWD) of 16mm was maintained throughout the welding process. The steel plate geometry and the process setup used to fabricate the weld samples are shown in Figure 1.

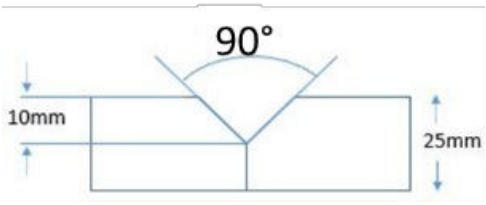

(a)

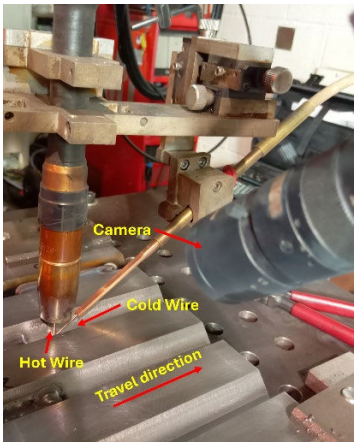

(b)

Figure 1. CWGMAW process setup. (a) Schematic view of joint configuration, (b) Welding setup

2.2 Energy Input

The energy input (EI) in J/mm, was calculated using Equation [1] according to ISO/TR 17671-1:2002(E) [4].

$$EI = \frac{\eta_a V I}{\upsilon_t} \quad [1]$$

where V, I, and υ_t are voltage, current and welding travel speed respectively. η_a is the arc efficiency, which depends on the welding process. An arc efficiency of 0.8 was used for GMAW.

2.3 Deposition Rate and Material Feed Rate

The deposition rate (DR) in Kg/hr, was calculated using Equation [2] as reported by Joao *et al*., 2023 [5].

$$DR = \rho\, \pi \frac{d^2}{4}\, (\upsilon_h + \upsilon_c) \quad [2]$$

Where ρ is the density of the welding electrode, which for the ER70S-6 wire is 7833.4 kg/m^3 [5]; d is the diameter of the wire (1.2mm for both hot and cold wires), υ_h and υ_c are the wire feed speed (WFS) of the hot and cold wires respectively.

The material feed rate (MFR) was calculated using Equation [3], following Joao *et al*., 2023 [5].

$$MFR = \frac{\upsilon_h + \upsilon_c}{\upsilon_t} \quad [3]$$

A constant MFR was maintained throughout the welding process.

2.4 Macrostructural and Microstructural Examination

After the welding, the specimens were cut in the transverse cross sections for macrostructural and microstructural examination using standard metallographic techniques. That is by grinding and polishing to mirror finish and etching with Nital 2% solution. The Macrographs were taken using a Nikon Optiphot-66 optical microscope, and the Image J processing and analysis software was used to measure the output as shown in Figure 2. Following this step for every sample, the assessment of the area of the heat affected zone were carried out.

The microstructural changes along the HAZ were analysed using the micrographs obtained from a Zeiss AxioLab5 optical microscope and a TESCAN scanning electron microscope.

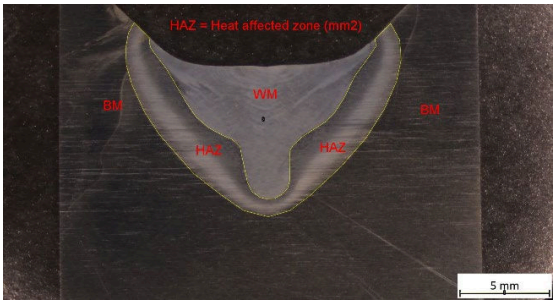

Figure 2. Macrograph of the sample showing the weld zones and the outlined HAZ

2.5 Microhardness Test

To analyse the microhardness variation along the weld samples, two transverse samples from each weld (CW0, CW5 and CW10) were extracted. A 300gf load was applied for a dwell time of 10 seconds per indentation using an INNOVATEST Falcon 500 machine. 2 parallel runs were done and a 0.5mm spacing between the indentations was maintained for all the samples. In total, seventy-two (72) test points were examined per weld, with an average of 4 to 6 indents in the heat affected zone region. Figure 3 depicts the hardness measurement mapping along a weld sample.

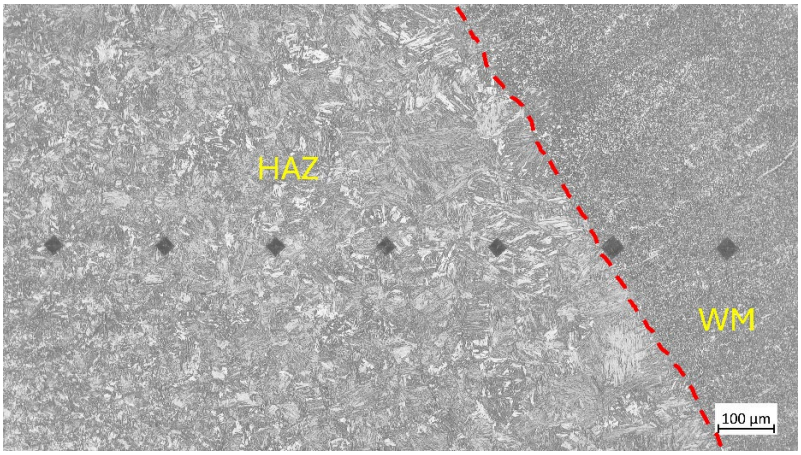

Figure 3. Microhardness mapping along the heat affected zone (HAZ), and weld metal (WM) of a typical weld prepared by CW-GMAW. The red dotted line represents the fusion line.

3. Results

3.1 Heat Input and Deposition Rate

The thermal control represented in Figure 4a shows a decrease in the heat input (EI) as the cold wire feed rate (CWFR) increases. This is largely due to the increase in the welding travel speed (υ_t), that was proportionally matched with the CWFR to maintain the same material feed rate (MFR) of all the weld samples; CW0, CW5 and CW10.

It can be seen in Figure 4b, that the deposition rate (DR) significantly increases with the addition of cold wire while the hot wire feed rate (HWFR) which controls the arc energy, is kept constant. The DR was increased by 45.54% and 91.1% relative to the standard GMAW process (CW0), when the cold wire was fed at a rate of 5m/min (CW5) and 10m/min (CW10), respectively. This led to a marked increase in productivity and less damage to the material due to the low heat absorption.

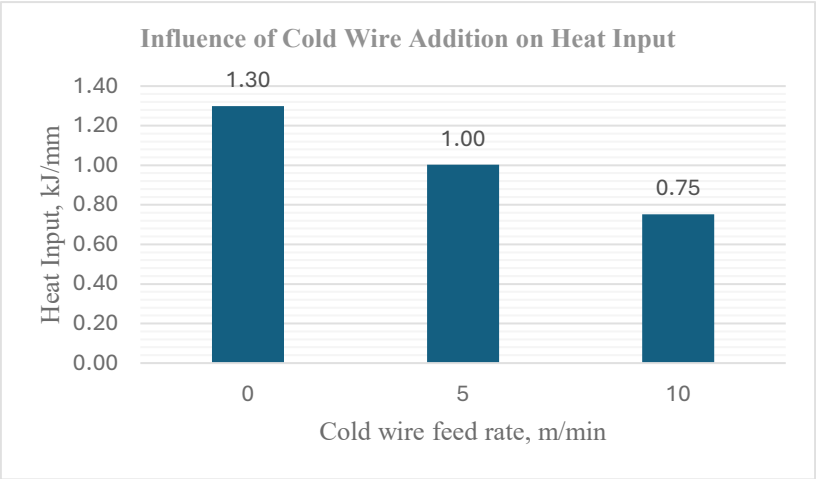

(a)

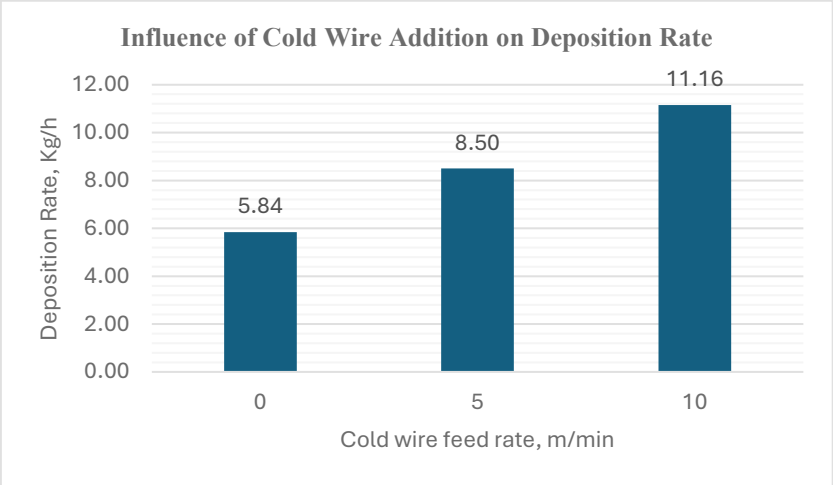

(b)

Figure 4. Influence of cold wire addition on; (a) Heat input, KJ/mm, and (b) Deposition rate, Kg/h

3.2 Macrostructure and Microstructure

The weld samples CW0, CW5 and CW10 were evaluated in terms of the size of heat affected zone (HAZ). The resultant HAZ area of the CW5 and CW10 samples was observed to be narrower than the HAZ of the CW0 sample. This was due to lower heat introduced to the weldment by cold-wire addition and the corresponding welding travel speed resulting in a faster cooling rate. The reduction in the HAZ size was larger for the CW10 sample due to the higher cold wire feeding rate (CWFR) of 10m/min. Macrographs of the three weld samples showing the measured HAZ area are shown in Figure 5.

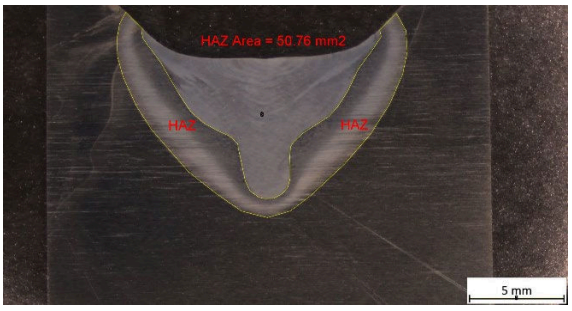

(a)

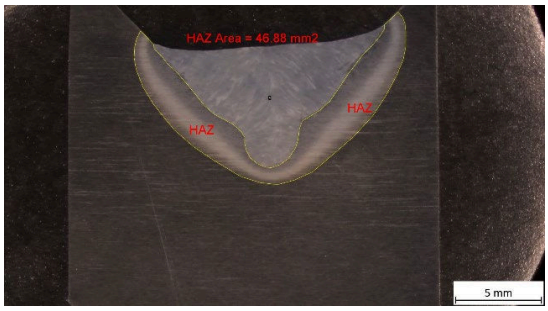

(b)

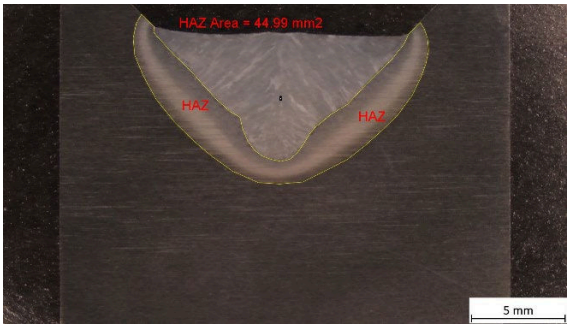

(c)

Figure 5. Macrographs of welded samples. (a) CW0; (b) CW5 and (c) CW10.

The results of the three welds geometry measurements indicated a reduction in the HAZ area from 50.76 ± 0.53 mm^2 for the CW0 weld to 46.88 ± 0.50 mm^2 and 44.99 ± 0.53 mm^2 for the CW5 and CW10 welds, respectively.

The microstructure of S275JR structural steel (BM) consists of ferrite and pearlite grains. As shown in Figure 6a, the black zone represent pearlite, while the lighter-coloured areas represent ferrite. Figure 6b and 6c show the microstructure of the heat affected zone (coarse-grain heat affected zone, CGHAZ) and weld metal (WM) of the CW0 sample respectively. In the HAZ, a microstructure consisting of ferrite and lamellar pearlite phase formed, and in the WM, the microstructure is largely dominated by acicular ferrite (α_a), widmanstatten ferrite (α_w) and ferrite (α). To compare the microstructures between CW0, CW5 and CW10, SEM images are provided in Figures 7a-c.

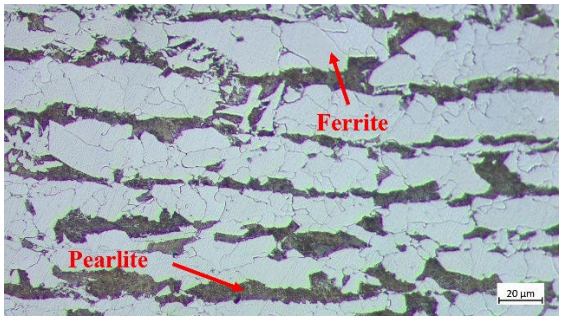

(a)

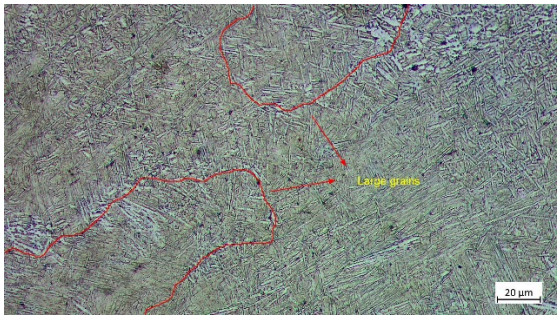

(b)

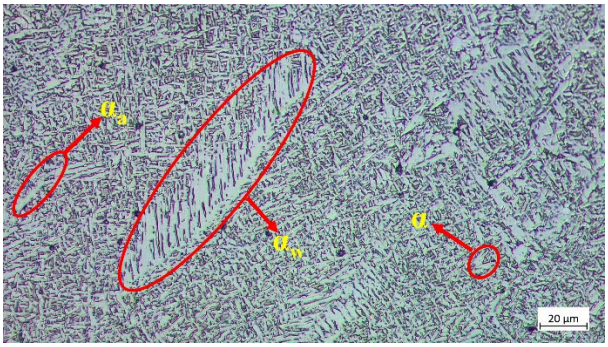

(c)

Figure 6. Optical micrographs of sample CW0; (a) base metal (BM); (b) coarse grain heat affected zone CGHAZ; and (c) weld metal (WM).

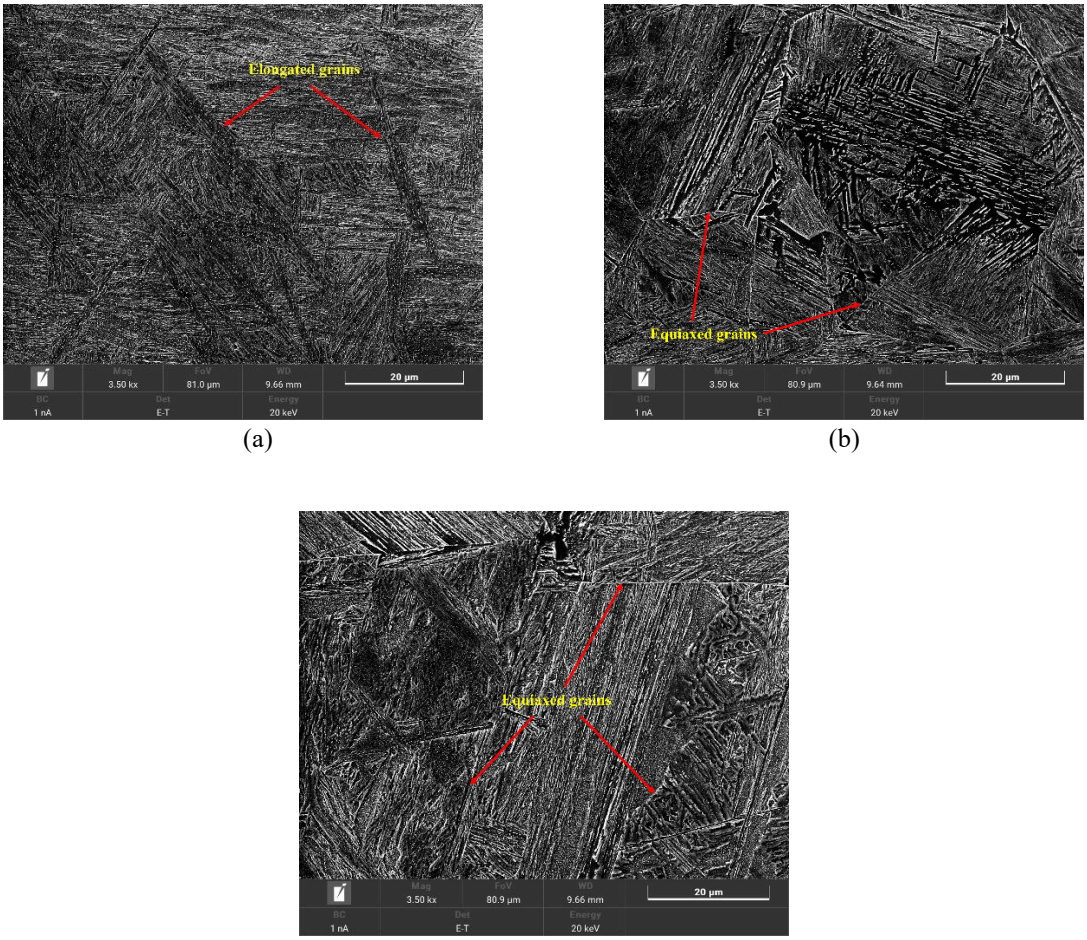

(a) (b)

(c)

Figure 7. SEM images showing HAZ of; (a) CW0; (b) CW5; and (c) CW10 weld samples.

3.3 Microhardness

Microhardness variations along the base metal (BM), heat affected zone (HAZ) and the weld metal (WM) are depicted in Figure 8. The microhardness value of the as-received base metal was measured as 194.94 ± 6 HV.

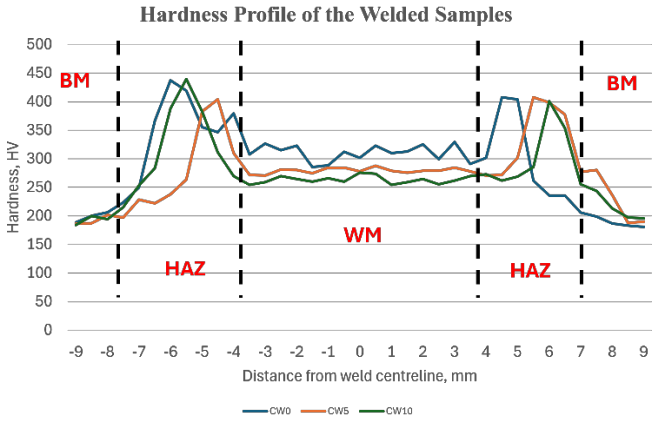

Figure 8. Hardness profile of the welded samples, CW0, CW5 and CW1

4. Discussion

The key findings of this investigation have demonstrated a clear relationship between cold wire feed rate (CWFR) and welding parameters, such as heat input, deposition rate, and the resulting microstructure, which further

influences the mechanical properties of the welded samples. The decrease in heat input with increasing CWFR agrees with findings from previous studies by Mohsen *et al*., 2017 [6], which emphasized the importance of reducing heat input to minimize thermal damage in high-strength low-alloy (HSLA) steels.

The macrostructures in Figure 5 revealed a significant decrease in the HAZ area with increased CWFR, which is a directly related to the low heat absorption and faster cooling rates. The reduction from 50.76 mm² in CW0 to 44.99 mm² in CW10 represents an improvement in the minimization of thermal damage induced in the material as shown in previous studies by Mohsen et al., 2017 [6]. In Figure 7a, the uneven distribution of elongated grains in the CW0 sample is an indication of high thermal gradients. In contrast, CW5 showed presence of primarily ferritic structures with finer grains indicating that the reduced heat input facilitated a homogenous distribution with slow cooling.

As shown in Figure 8, the average microhardness of the HAZ reduced from 383.90 HV to 380.06 HV by the addition of a cold wire in the CW5 sample relative to the CW0. However, the average microhardness in the HAZ increased to 386.78 HV when the cold wire was fed at 10m/min (CW10). The different influence of the cold-wire addition on the microhardness is attributed to the microstructural alterations taking place in the HAZ, due to changes in the actual welding heat input and consequent cooling rate.

5. Conclusion

This study investigated the influence of adding a cold wire during gas metal arc welding during repair of S275JR structural steel. The research is aimed at improving repair productivity through increased deposition rates at a reduced heat input. The results presented demonstrate that adding a cold wire during welding significantly increases productivity and material performance. The deposition rate was significantly increased up to 91% with respect to standard GMAW (no cold wire).

The results highlighted that the addition of cold wire is a promising approach in applications where thermal control and material performance are critical.

6. Acknowledgments

Zahraddeen Musa would like to thank the Welding and Additive Manufacturing Centre at Cranfield University, where this research was conducted. Funding for this project was provided by Petroleum Technology Development Fund in Nigeria, under the PTDF OSS scholarship scheme no. PTDF/OSS/20PHD123.

7. References

1. Yuhui, W., Liao, B., Ligang, L., Xianfeng, L., Hang, S., Caifu, Y. and Qingfeng, W. (2012). Effects of N and B on Continuous Cooling Transformation Diagrams of Mo–V–Ti Micro-alloyed Steels. Phase Transitions, 85 (5) 419–426. https://doi.org/10.1080/01411594.2011.611401

2. Sanchez, A., Ojeda, M., Gomez, H., Bermejo, C., Victor, M., Orlando, E., Jorge, B., Alvaro, M., Heriberto, M. and Julio, M. (2017). Review and analysis of repair/rehabilitation methods for natural gas pipelines. Proceedings of the ASME 2017 International Mechanical Engineering Congress and Exposition IMECE2017 November 3-9, 2017, Tampa, Florida, USA. IMECE2017-71543

3. Abbas, M.I. (2013). Girth welds fitness after multiple SMAW repairs. Pipeline Gas Journal, 240, 1.

4. ISO/TR 17671-1:2002(E); Welding—Recommendations for Welding of Metallic Materials—Part 1: General Guidance for Arc Welding. ISO (International Organization for Standardization): Geneva, Switzerland, 2002.

5. Bento, J.B., Wang, C., Ding, J., and Williams, S. (2023). Process Control Methods in Cold Wire Gas Metal Arc Additive Manufacturing. Metals 2023, 13, 1334. https://doi.org/10.3390/10.3390/met13081334.

6. Mohammadijoo, M., Kenny, S., Collins, L., Henein, H., and Ivey, D.G. (2017). Characterization of HAZ of API X70 Micro alloyed Steel Welded by Cold-Wire Tandem Submerged Arc Welding. Metallurgical and Materials Transactions A Volume 48A, MAY 2017. DOI: 10.1007/s11661-017-4041-x.